MATCH
Communications in Mathematical and in Computer Chemistry

MATCH Commun. Math. Comput. Chem. **93** (2025) 69–97
ISSN: 0340–6253
doi: 10.46793/match.93-1.069I

Numerical Computations of Time–Dependent Auto–Catalytic Glycolysis Chemical Reaction–Diffusion System

Mohammad Izadi[a,*], **Hijaz Ahmad**[b], **Hari Mohan Srivastava**[b,c,d,e,f,g]

[a] *Department of Applied Mathematics, Faculty of Mathematics and Computer, Shahid Bahonar University of Kerman, Kerman, Iran*
[b] *Section of Mathematics, International Telematic University Uninettuno, Corso Vittorio Emanuele II, 39,00186 Roma, Italy*
[c] *Department of Mathematics and Statistics, University of Victoria, Victoria, British Columbia V8W 3R4, Canada*
[d] *Department of Medical Research, China Medical University Hospital, China Medical University, Taichung 40402, Taiwan*
[e] *Department of Mathematics and Informatics, Azerbaijan University, 71 Jeyhun Hajibeyli Street, AZ1007 Baku, Azerbaijan*
[f] *Center for Converging Humanities, Kyung Hee University, 26 Kyungheedae-ro, Dongdaemun-gu, Seoul 02447, Republic of Korea*
[g] *Department of Applied Mathematics, Chung Yuan Christian University, Chung-Li, Taoyuan City 320314, Taiwan*
izadi@uk.ac.ir, ahmad.hijaz@uninettuno.it, harimsri@math.uvic.ca

(Received January 9, 2024)

Abstract

A combined semi-discretized spectral matrix collocation algorithm based on (new) family of Krawtchouk polynomials is proposed to solve the time-dependent nonlinear auto-catalytic glycolysis reaction-diffusion system arising in mathematical chemistry. The

*Corresponding author.

first stage of the numerical algorithm is devoted to the Taylor series time advancement procedure yielding to a (linear and steady) system of ODEs. In the second stage and in each time frame, a matrix collocation technique based on the Krawtchouk polynomials is utilized to the resulting system of ODEs in an iterative manner. The results of the performed numerical experiments with Neumann boundary conditions are given to show the utility and applicability of the combined Taylor-Krawtchouk spectral collocation algorithm. The positive property of the glycolysis chemical model is sustained by the proposed algorithm and verified through comparisons with existing numerical methods in the literature. The combined technique is simple and flexible enough to easily produce the approximate solutions of diverse physical and applied models in engineering and science.

1 Introduction

Partial differential equations (PDEs) have a range of applications in diverse disciplines in applied sciences. In chemical engineering many chemical reaction models can be described mathematically based on physical knowledge. Glycolysis is a series of reactions that convert glucose to pyruvate. The widespread occurrence of glycolysis in other species shows that it is an ancient metabolic pathway [26]. Indeed, the glycolysis model is a special kind of the autocatalytic reaction and has been expressed mathematically in the form of chemical reaction systems [9, 10, 23].

Sel'kov was the first one who proposed a mathematical model for glycolysis [27]. This model consists of two (first-order) ordinary differential equations (ODEs) given by the coupled form [30]

$$\begin{cases} \dfrac{du(\tau)}{d\tau} = -u(\tau) + \sigma\, v(\tau) + u^2(\tau)\, v(\tau), \\ \dfrac{dv(\tau)}{d\tau} = \lambda - \sigma\, v(\tau) - u^2(\tau)\, v(\tau). \end{cases} \tag{1}$$

Here, two kinetic parameters σ and λ are non-negative. This (dimensionless) model studied and discussed numerically by Mickens [21]. He employed the nonstandard finite difference method (FDM), which preserves the positiveness of the chemical concentrations u and v. As shown in [30, pp. 205-209], the equilibrium of the system (2) is given in the form

$(u_*, v_*) = (\lambda, \frac{\lambda}{\lambda^2+\sigma})$. By defining the parameter $\kappa = -\frac{\lambda^4+\lambda^2(2\sigma-1)+\sigma+\sigma^2}{\lambda^2+\sigma}$, it is also proved this equilibrium point is stable if $\kappa < 0$ and unstable if $\kappa > 0$.

Based on the above glycolysis model (1), some research works have been conducted to generalize the mathematical models of the chemical reaction-diffusion (RD) systems with more than two variables. In [35], the authors investigated a general form of glycolysis RD system and the issues of existence of non-constant steady state solutions as well as the time-periodic orbits examined. The steady-state bifurcation for a two species glycolysis RD system studied in [33]. The chief aim of this research study is to solve a nonlinear system of two PDEs known as the auto-catalytic glycolysis model equation in the form

$$\begin{cases} \dfrac{\partial u(\chi,\tau)}{\partial \tau} - d_u \dfrac{\partial^2 u(\chi,\tau)}{\partial \chi^2} = -u(\chi,\tau) + \sigma\, v(\chi,\tau) + u^2(\chi,\tau)\, v(\chi,\tau), \\ \dfrac{\partial v(\chi,\tau)}{\partial \tau} - d_v \dfrac{\partial^2 v(\chi,\tau)}{\partial \chi^2} = \lambda - \sigma\, v(\chi,\tau) - u^2(\chi,\tau)\, v(\chi,\tau), \end{cases} \tag{2}$$

for $(\chi, \tau) \in D \times D_T$ where $D := (0, 1)$ and $D_T := (0, T)$. The given initial conditions are

$$u(\chi, \tau = 0) = f(\chi) > 0, \quad v(\chi, \tau = 0) = g(\chi) > 0, \quad \chi \in D. \tag{3}$$

Here, $u = u(\chi, \tau)$ and $v = v(\chi, \tau)$ represent the chemical concentrations of two chemicals at time τ and f, g are two (smooth) given functions. Moreover, d_u and d_v denote the diffusion coefficients and assumed to be positive constants. The supplemented Neumann boundary conditions are homogeneous given by

$$\begin{cases} \dfrac{\partial u}{\partial \chi}(\chi = 0, \tau) = 0, \quad \dfrac{\partial u}{\partial \chi}(\chi = 1, \tau) = 0, \\ \dfrac{\partial v}{\partial \chi}(\chi = 0, \tau) = 0, \quad \dfrac{\partial v}{\partial \chi}(\chi = 1, \tau) = 0, \end{cases} \quad \tau \in D_T. \tag{4}$$

Over the past decades, some research works have been devoted in the

literature to deal numerically with the chemical reaction-diffusion (RD) systems (2) and its related models. In [18] the Gray-Scott autocatalysis system solved by a combination of exponential B-spline collocation scheme and the sinc differential quadrature procedure. The numerical solutions of RD Brusselator system obtained by different numerical procedures in [2, 11, 22, 32]. Positivity preserving numerical models based on nonstandard FDMs have been developed in the works [3, 5, 6]. Some other existing computational techniques based on spectral collocation strategies related to reaction-diffusion and Brusselator system can be found in [8, 15, 16, 31].

The main purpose of the current study is to examine a novel combined computational approach to approximate the chemical concentrations of the RD system (2). The proposed spectral algorithm is not only straightforward in implementation stage but retain also the positiveness of the solutions and the stability of equilibrium point (u_*, v_*). In this respect, we first employ the Taylor series formula to get rid of the intrinsic nonlinearity of the system. This allows us to advance in time by solving a family of (steady-state) linear system of ODEs rather than a nonlinear system of PDE. Secondly, we solve the resultant systems of ODEs by employing a spectral matrix collocation method based on the novel polynomial basis functions known as Krawtchouk polynomials, see [7, 19]. We further establish the upper bound for the error norm in the L_2 norm. To the best of authors' knowledge, this is the first time the combined Taylor-Krawtchouk collocation approach is applied to the underlying model problem (2). We also emphasize that the spectral collocation procedures based on diverse types of polynomial families have been successfully applied to important mathematical models over the last decades. Let us mention some of them such as clique, Fibonacci, Morgan-Voyce, Legendre, Chebyshev, and airfoil polynomials. More details can be found in the published works [1, 4, 13, 14, 17, 25, 28, 34].

The plan of this research study is organized next. Some preliminary facts on Krawtchouk polynomials are provided in Section 2. The convergence analysis and error bound of this family of functions are then established in a weighted L_2 norm. The time-marching algorithm based on the Taylor series expansion is described in Section 3. The main combined

approximation algorithm called Taylor-Krawtchouk collocation technique is illustrated in detail in Section 4. Numerical experiments and MATLAB plots have been provided in Section 5 to describe the main results derived in this study. A conclusion is given in the last Section 6.

2 The Krawtchouk polynomials: A convergence analysis

The main aim is to first review the definition of Krawtchouk polynomials (KPs). Then, we are interested to mention some main properties of them. Finally, the convergence analysis of KPs in the sense of approximation theory is studied.

2.1 An overview of Krawtchouk polynomials

The definition of Krawtchouk polynomials (KPs) was traced back to a Ukrainian mathematician Mikhail Krawtchouk who introduced them in 1929. The importance of the KPs has been found in many applications in discrete mathematics and in particular in coding theory [7]. Among others, finding the integral zeros of KPs is a hot topic among combintorics [19]. For more applications, we refer the readers to [12, 20, 24].

Let $N \in \mathbb{N}$ and $q > 1$ be a real number. The q-ray KPs $\mathbb{K}_{i,N}(\chi) \equiv \mathbb{K}_i(\chi; q, N)$ of degree $i \leqslant N$ and with two parameters q and N satisfy the following generating function

$$\sum_{i=0}^{\infty} \mathbb{K}_{i,N}(\chi)\, w^i = [1-w]^{\chi}\, [1+(q-1)w]^{N-\chi}, \quad \chi \in \mathbb{R}.$$

As stated in the book [29, p. 75, Eq. 1.9 (2)], the Krawtchouk polynomials are, in essence, a hypergeometric polynomial given by

$$\mathbb{K}_i(\chi; q, N) := {}_2F_1\left(-i, -\chi; -N; \frac{1}{q}\right),$$

where $0 < q < 1$ and $\chi = 0, 1, \cdots, N$. In particular, for the binary case

$q = 2$ in the generating function, we get

$$\sum_{i=0}^{\infty} \mathbb{K}_{i,N}(\chi)\, w^i = (1-w)^{\chi}\ (1+w)^{N-\chi}, \quad \chi \in \mathbb{R}.$$

Below, we restrict the discussions only for the binary case. For $q \neq 2$, we may refer to [7, 24].

Definition 1. The (binary) Krawtchouk polynomials are defined explicitly as

$$\mathbb{K}_{i,N}(\chi) := \sum_{j=0}^{i} (-1)^j \binom{\chi}{j} \binom{N-\chi}{i-j} = \sum_{j=0}^{i} (-2)^j \binom{\chi}{j} \binom{N-j}{i-j}, \quad (5)$$

where

$$\binom{\chi}{j} := \frac{\chi(\chi-1)(\chi-2)\ldots(\chi-j+1)}{j!}, \quad \binom{\chi}{0} := 1, \quad \binom{\chi}{1} := 1.$$

It can be easily verified that $\mathbb{K}_{0,N}(\chi) := 1$ and $\mathbb{K}_{1,N}(\chi) := N - 2\chi$. Besides two explicit forms given in (5) we may obtain the KPs by the following recursive formula

$$\mathbb{K}_{i+1,N}(\chi) = \frac{N-2\chi}{i+1}\, \mathbb{K}_{i,N}(\chi) - \frac{N-i+1}{i+1}\, \mathbb{K}_{i-1,N}(\chi), \quad i \geqslant 1. \quad (6)$$

For specific values of $i = 1, 2, 3$ in (6) we get the list of KPs

$$\begin{aligned}
\mathbb{K}_{2,N}(\chi) &= 2\chi^2 - 2N\,\chi + (N^2 - N)/2, \\
\mathbb{K}_{3,N}(\chi) &= -\frac{4}{3}\,\chi^3 + 2N\,\chi^2 - (N^2 - N + \frac{2}{3})\chi + (N^3 - 3N^2 + 2N)/6, \\
\mathbb{K}_{4,N}(\chi) &= \frac{2}{3}\,\chi^4 - \frac{4}{3}N\,\chi^3 + (N^2 - N + \frac{4}{3})\chi^2 - (\frac{N^3}{3} - N^2 + \frac{4N}{3})\chi \\
&\quad + (N^4 - 6N^3 + 11N^2 - 6N)/24.
\end{aligned}$$

One can evidently realize that $\mathbb{K}_{i,N}(0) = \binom{N}{i}$ for all $i \in \mathbb{N}$. We also have $\mathbb{K}_{i,K}(1) = (1 - \frac{2i}{N})\binom{N}{i}$.

The next result is about the orthogonality of the sequence $\{\mathbb{K}_{i,N}\}_{i=0}^{N}$. Let δ_{ij} denotes the well-known Kronecker delta function. The family of

KPs constitutes a sequence of discrete orthogonal functions in the sense that

$$\sum_{\ell=0}^{N} \mathbb{K}_{i,N}(\ell)\, \mathbb{K}_{j,N}(\ell) \binom{N}{\ell} = \delta_{ij} \binom{N}{i} 2^N, \quad \sum_{\ell=0}^{N} \mathbb{K}_{j,N}(\ell)\, \mathbb{K}_{\ell,N}(i) = \delta_{ji} 2^N. \tag{7}$$

To investigate the error analysis of KPs from the point of approximation theory, we need the following decomposition for the vector of KPs. Denote I as a positive integer. We form the vector of $(I+1)$ KPs defined by

$$\boldsymbol{K}_I(\chi) := \begin{bmatrix} \mathbb{K}_{0,N}(\chi) & \mathbb{K}_{1,N}(\chi) & \dots & \mathbb{K}_{I,N}(\chi) \end{bmatrix}. \tag{8}$$

Lemma 1. *The next decomposition for the vector $\boldsymbol{K}_I(\chi)$ is valid*

$$\boldsymbol{K}_I(\chi) = \boldsymbol{\Delta}_I(\chi)\, \boldsymbol{P}_I, \tag{9}$$

where the vector $\boldsymbol{\Delta}_I(\chi)$ is as follows

$$\boldsymbol{\Delta}_I(\chi) = \begin{bmatrix} 1 & \chi & \chi^2 & \dots & \chi^I \end{bmatrix}.$$

Also, the structured matrix $\boldsymbol{P}_I$ is a upper-triangular matrix whose element are constant. The size of matrix $\boldsymbol{P}_I$ is $(I+1)$ by $(I+1)$ and defined as

$$\boldsymbol{P}_I = \begin{bmatrix} p_{0,0}^N & p_{1,0}^N & p_{2,0}^N & \dots & p_{I-1,0}^N & p_{I,0}^N \\ 0 & p_{1,1}^N & p_{2,1}^N & \dots & p_{I-1,1}^N & p_{I,1}^N \\ 0 & 0 & p_{2,2}^N & \dots & p_{I-1,2}^N & p_{I,2}^N \\ \vdots & \vdots & \ddots & \ddots & \ddots & \vdots \\ 0 & 0 & 0 & \dots & p_{I-1,I-1}^N & p_{I,I-1}^N \\ 0 & 0 & 0 & \dots & 0 & p_{I,I}^N \end{bmatrix}.$$

Here, the entries of $\boldsymbol{P}_I$ have the forms

$$
\begin{aligned}
p_{i,i}^N &:= \frac{(-2)^i}{i!}, \quad i = 0, 1, \ldots, I, \\
p_{i,i-1}^N &:= \frac{(-2)^{i-1} N}{(i-1)!}, \quad i = 1, 2, \ldots, I, \\
p_{i,i-2}^N &:= \frac{(-2)^{i-2}}{6(i-2)!} \left(3N^2 - 3N + 2i - 4\right), \quad i = 2, 3, \ldots, I, \\
p_{i,i-3}^N &:= \frac{(-2)^{i-3} N}{6(i-3)!} \left(N^2 - 3N + 2i - 4\right), \quad i = 3, 4, \ldots, I,
\end{aligned}
$$

and so on.

Proof. The proof of this Lemma will be deduced by using the induction on I, the explicit representation (5), and the fact that each $\mathbb{K}_{i,N}(\chi)$ can be written in a polynomial format as

$$
\mathbb{K}_{i,N}(\chi) = p_{i,i}^N \chi^i + p_{i,i-1}^N \chi^{i-1} + p_{i,i-2}^N \chi^{i-2} + \ldots + p_{i,1}^N \chi + p_{i,0}^N,
$$

for $i = 1, \ldots, I$. ■

It is worth mention that the matrix $\boldsymbol{P}_I$ is nonsingular as one can see that $\det(\boldsymbol{P}_I) = \frac{(-2)^{I(I+1)/2}}{1!2!\ldots I!}$.

2.2 Convergence analysis and error bound estimation

In this work the family of KPs will be used on the interval $D_X = [0, X]$, where usually $X = 1$ is taken. It is very important to have convergence when a function is expanded in terms of these KPs. To proceed, one requires to define an appropriate function space on $[0, X]$. Let us consider the space

$$
L_w^2[0, X] := \{q : [0, X] \to \mathbb{R} \,:\, q \text{ is measurable and } \|q\|_w < \infty\}, \; w(\chi) = \frac{1}{X}.
$$

Note that the related induced norm is defined by $\|q\|_w^2 := \int_0^X |q(\chi)|^2 w(\chi) d\chi$.

We suppose that a given function $q(\chi)$ belongs to the space $L_w^2[0, X]$. By approximating the function $q(\chi)$ in a series format as a combination of

KPs we arrive at

$$q(\chi) = \sum_{i=0}^{\infty} \psi_i \, \mathbb{K}_{i,N}(\chi), \quad \chi \in [0, X]. \tag{10}$$

Here, the coefficients ψ_i, $i \geqslant 0$ are being unknown and have to determined. Working with an infinite series expansion is not practical. Therefore, we pay attention to a finite-dimensional subspace $\mathbb{Y}_I \subseteq L_w^2[0, X]$ spanned as follows

$$\mathbb{Y}_I := \mathrm{Span}\langle \mathbb{K}_{0,N}(\chi), \mathbb{K}_{1,N}(\chi), \ldots, \mathbb{K}_{I,N}(\chi) \rangle.$$

Evidently, the subspace $\mathbb{Y}_I$ is of finite-dimensional $I + 1$ and therefore a closed subspace of $L_w^2[0, X]$. The next conclusion is that it is a complete subspace of $L_w^2[0, X]$. This implies that one finds the closet (best) approximation element $q^\star(\chi) \in \mathbb{Y}_I$ such that

$$\|q(\chi) - q^\star(\chi)\|_w \leqslant \|q(\chi) - z(\chi)\|_w, \quad \forall z \in \mathbb{Y}_I.$$

We practically utilize only the first $(I + 1)$ KPs to approximate $q(\chi)$ as previously stated. It follows that

$$q(\chi) \approx q_I^N(\chi) := \sum_{i=0}^{I} \psi_i \, \mathbb{K}_{i,N}(\chi), \quad \chi \in [0, X]. \tag{11}$$

It is possible to represent the approximate solution $q_I^N(\chi)$ in a compact format as follows

$$q_I^N(\chi) = \boldsymbol{K}_I(\chi) \, \boldsymbol{\Psi}_I, \tag{12}$$

where $\boldsymbol{K}_I(\chi)$ is defined in (8). Besides, the vector of unknowns ψ_i for $i = 0, 1, \ldots, I$ is defined by

$$\boldsymbol{\Psi}_I := \begin{bmatrix} \psi_0 & \psi_1 & \ldots & \psi_I \end{bmatrix}^t.$$

In the next result we assert that by increasing the number of bases I, the difference between $q(\chi)$ and the approximation $q_I^N(\chi)$ in the series

form (11) goes to zero. Thus, we define the error term $E_I(\chi) := q(\chi) - q_I^N(\chi)$ for convenience.

Theorem 1. *We assume that* $q(\chi) \in L_w^2[0,X] \cap C^{I+1}[0,X]$ *and let* $q_I^N(\chi) = \boldsymbol{K}_I(\chi)\,\boldsymbol{\Psi}_I$ *be the (closet) best approximation to* $q(\chi)$ *out of space* $\mathbb{Y}_I$. *Then,* $E_I(\chi)$ *converges to zero as* $I \to \infty$. *Indeed, we have*

$$\|E_I(\chi)\|_2 \leqslant \frac{\sqrt{2}\,q_\infty\,X_0^{I+\frac{2}{3}}}{\sqrt{X(2I+3)}\,(I+1)!}, \quad q_\infty := \max_{\chi\in[0,X]}\left|q^{(I+1)}(\chi)\right|, \tag{13}$$

where $X_0 := \max\{\chi_0, X-\chi_0\}$ *for a* $\chi_0 \in (0,X)$.

Proof. Let us fix an arbitrary real number $\chi_0 \in [0,X]$. Since $q(\chi) \in C^{I+1}[0,X]$, we can write $q(\chi)$ in terms of its Taylor series expansion about χ_0. The resulting expansion is

$$q(\chi) = Q_I(\chi) + R_I(\chi),$$

where $Q_I(\chi) := \sum_{m=0}^{I} q^{(m)}(\chi_0)(\chi-\chi_0)^m/m!$ and $R_I(\chi) := q^{(I+1)}(t_0)(\chi-\chi_0)^{I+1}/(I+1)!$ for some point t_0 between $(0,\chi_0)$ or (χ_0,X). In particular, for the Taylor remainder error term $R_I(\chi)$ we have

$$|R_I(\chi)| = |q(\chi) - Q_I(\chi)| \leqslant \frac{(\chi-\chi_0)^{I+1}\,q_\infty}{(I+1)!}, \quad \forall \chi \in [0,X]. \tag{14}$$

We then apply the fact that $q_I^N(\chi)$ shows the closet approximation to $q(\chi)$ out of $\mathbb{Y}_I$. Based on the above discussion, one finds that

$$\|q(\chi) - q_I^N(\chi)\|_w \leqslant \|q(\chi) - z(\chi)\|_w, \quad \forall z \in \mathbb{Y}_I. \tag{15}$$

The foregoing inequality (15) is still valid for a specific selection for $z(\chi)$ to be $Q_I(\chi)$. Therefore, we conclude

$$\|q(\chi) - q_I^N(\chi)\|_w^2 \leqslant \|q(\chi) - Q_I(\chi)\|_w^2 = \int_0^X |q(\chi) - Q_I(\chi)|^2\, w(\chi)d\chi.$$

Owing to (14) and using the definition of the error term we reach at

$$\|E_I(\chi)\|_w^2 \leqslant \Big[\frac{q_\infty}{(I+1)!}\Big]^2 \int_0^X (\chi-\chi_0)^{2I+2}\, w(\chi) d\chi. \tag{16}$$

We now need to estimate the value of the definite integral. It can be computed exactly as

$$\int_0^X (\chi-\chi_0)^{2I+2}\, w(\chi) d = \frac{1}{X(2I+3)}\left[(\chi-\chi_0)^{2I+3}\right]\Big|_{\chi=0}^{\chi=X} \leqslant \frac{2X_0^{2I+3}}{X(2I+3)}.$$

After placing the upper bound for the integral into (16) followed by performing the square root we arrive at the aimed result. ■

We remark that if we choose $X = 1$ in the computation, the the obtained upper bound in (13) will reduce to $\|E_I(\chi)\|_2 \leqslant \frac{\sqrt{2}\, q_\infty}{\sqrt{(2I+3)}\,(I+1)!}$. In either case, we immediately conclude that the error term goes to zero as I approaching to the infinity.

3 The method of time-marching procedure

In order to discretize the system of PDEs (2) in time variable, we employ the Taylor series approach. Towards this end, we first set up a (uniform) mesh of the interval $[0, T]$ into S subdivisions. Denote the mesh by $\mathbb{T}_h := \{\tau_s\}_{s=0}^S$ with nodes $\tau_s = sh$ such that $\tau_0 = 0$, $\tau_S = T$, and $h = \tau_s - \tau_{s-1}$ for $s = 1, 2, \ldots, S$.

Let us denote by u_s, v_s the approximations related to the exact solutions $u(\chi, \tau), v(\chi, \tau)$ of system (2) at time frame τ_s respectively. Thus, we have

$$u_s \equiv u_s(\chi) := u(\chi, \tau_s), \quad v_s \equiv v_s(\chi) := v(\chi, \tau_s), \quad \chi \in D.$$

We proceed by evaluating the two equations in (2) at time level τ_s to get

$$\begin{cases} \dfrac{\partial u_s}{\partial \tau} = d_u \dfrac{\partial^2 u_s}{\partial \chi^2} - u_s + \sigma\, v_s + u_s^2\, v_s, \\ \dfrac{\partial v_s}{\partial \tau} = d_v \dfrac{\partial^2 v_s}{\partial \chi^2} + \lambda - \sigma\, v_s - u_s^2\, v_s. \end{cases} \tag{17}$$

The applications of the Taylor series formula reveal that

$$\begin{cases} \dfrac{\partial u_s}{\partial \tau} = \dfrac{1}{h}(u_{s+1} - u_s) - \dfrac{h}{2} \dfrac{\partial^2 u_s}{\partial \tau^2} + \mathcal{O}(h^2), \\ \dfrac{\partial v_s}{\partial \tau} = \dfrac{1}{h}(v_{s+1} - v_s) - \dfrac{h}{2} \dfrac{\partial^2 v_s}{\partial \tau^2} + \mathcal{O}(h^2). \end{cases} \tag{18}$$

From these formulae we can also approximate the first-order derivatives $\frac{\partial u_s}{\partial \tau}$ and $\frac{\partial v_s}{\partial \tau}$ by the difference quotients $(u_{s+1} - u_s)/h$, $(v_{s+1} - v_s)/h$ respectively. The next job is to differentiate (17) with regard to τ and replacing all τ-derivatives by the above difference quotients. The resulting formulations are

$$\begin{cases} h \dfrac{\partial^2 u_s}{\partial \tau^2} & = d_u\left(\dfrac{\partial^2 u_{s+1}}{\partial \chi^2} - \dfrac{\partial^2 u_s}{\partial \chi^2}\right) - (u_{s+1} - u_s) + \sigma\,(v_{s+1} - v_s) \\ & \quad + 2u_s\, v_s (u_{s+1} - u_s) + u_s^2\,(v_{s+1} - v_s), \\ h \dfrac{\partial^2 v_s}{\partial \tau^2} & = d_v\left(\dfrac{\partial^2 v_{s+1}}{\partial \chi^2} - \dfrac{\partial^2 v_s}{\partial \chi^2}\right) - \sigma\,(v_{s+1} - v_s) - 2u_s\, v_s (u_{s+1} - u_s) \\ & \quad - u_s^2\,(v_{s+1} - v_s). \end{cases} \tag{19}$$

We now replace the two second-order derivatives in (18) by the above two relevant formulae. Also, we substitute the involved first-order derivatives on the left-hand sides of (18) by the corresponding relations in (17). Hence, we do some manipulations and collecting the same terms together. We finally gain a discretized set of equations in a linear form for (2). Let us introduce the notations

$$\boldsymbol{Z}_{s+1}(\chi) := \begin{bmatrix} u_{s+1}(\chi) \\ v_{s+1}(\chi) \end{bmatrix}, \quad \boldsymbol{N}_{s,1}(\chi) := \begin{bmatrix} -h\, d_u & 0 \\ 0 & -h\, d_v \end{bmatrix},$$

$$\boldsymbol{R}_s(\chi) := \begin{bmatrix} (2-h)u_s(\chi) + h\, d_u\, \frac{d^2}{d\chi^2} u_s(\chi) + h\, v_s(\chi)\left(\sigma - u_s^2(\chi)\right) \\ (2-\sigma h)v_s(\chi) + 2\lambda\, h + h\, d_v\, \frac{d^2}{d\chi^2} v_s(\chi) + h\, v_s(\chi)\, u_s^2(\chi) \end{bmatrix},$$

and

$$\boldsymbol{N}_{s,2}(\chi) := \begin{bmatrix} 2 + h\,(1 - 2\,u_s(\chi)\, v_s(\chi)) & -h\,\sigma \\ 2h\, u_s(\chi)\, v_s(\chi) & 2 + h\left(\sigma + u_s^2(\chi)\right) \end{bmatrix}.$$

In the matrix representation format and with aid of the aforementioned notations we have

$$\boldsymbol{N}_{s,1}(\chi)\frac{d^2}{d\chi^2}\boldsymbol{Z}_{s+1}(\chi) + \boldsymbol{N}_{s,2}(\chi)\,\boldsymbol{Z}_{s+1}(\chi) = \boldsymbol{R}_s(\chi), \quad s = 0, 1, \ldots, S-1. \tag{20}$$

It is evident that we now must solve a sequence of linear second-order differential equations in (20). To calculate the approximate solution of (20), we need the vector $\boldsymbol{Z}_0(\chi)$, which is clearly obtained from the initial conditions $u_0(\chi) = f(\chi)$ and $v_0(\chi) = g(\chi)$. In addition to these functions, the second-order derivative of them are also appeared in the vector function $\boldsymbol{R}_0(\chi)$. The Neumann boundary conditions (4) can be also converted accordingly. The matrix forms of them at $\chi = 0, 1$ are given next

$$\frac{d}{d\chi}\boldsymbol{Z}_{s+1}(0) = \boldsymbol{C}_{s+1}^0 := \begin{bmatrix} 0 \\ 0 \end{bmatrix}, \quad \frac{d}{d\chi}\boldsymbol{Z}_{s+1}(1) = \boldsymbol{C}_{s+1}^1 := \begin{bmatrix} 0 \\ 0 \end{bmatrix}. \tag{21}$$

4 Description of the main Taylor-Krawtchouk collocation methodology

By solving the sequence of discretized equations (20) together with the Neumann boundary conditions (21) we get the approximate solutions of the auto-catalytic system (2). By setting $s = 0$ in (20) and by using $\boldsymbol{Z}_0(\chi)$ we have to solve it for the approximate solution $\boldsymbol{Z}_1(\chi)$ at time frame $\tau_1 = h$. In the next iteration we will use $\boldsymbol{Z}_1(\chi)$ as the coefficients of (20) and solve it for $\boldsymbol{Z}_2(\chi)$ at time level $\tau_2 = 2h$ and so on.

To continue, let assume that the approximate solution of (20) at time

frame $s-1$ will be available for $s \geqslant 1$. Now, the assumption is that at the next time frame s one can write the approximate forms for the solutions of system (20) as a summation of $(I+1)$ Krawtchouk basis functions as

$$\begin{cases} u_s(\chi) \approx u_{s,I}^N(\chi) = \sum_{i=0}^{I} \psi_{i,u}^{(s)}\, \mathbb{K}_{i,N}(\chi), \\ v_s(\chi) \approx v_{s,I}^N(\chi) = \sum_{i=0}^{I} \psi_{i,v}^{(s)}\, \mathbb{K}_{i,N}(\chi). \end{cases} \tag{22}$$

To determine the former approximations we must find the coefficients $\psi_{i,w}^{(s)}$ for $w = u, v$ and $i = 0, 1, \ldots, I$. For brevity, let us insert these unknowns in the following vector formats

$$\boldsymbol{\Psi}_{I,w}^{(s)} := \begin{bmatrix} \psi_{0,w}^{(s)} & \psi_{1,w}^{(s)} & \ldots & \psi_{I,w}^{(s)} \end{bmatrix}^t, \quad w = u, v.$$

The vector of KPs bases formed previously as $\boldsymbol{K}_I(\chi)$ in (8). By using it we may rewrite the former equations (22) as

$$\begin{cases} u_{s,I}^N(\chi) = \boldsymbol{K}_I(\chi)\, \boldsymbol{\Psi}_{I,u}^{(s)}, \\ v_{s,I}^N(\chi) = \boldsymbol{K}_I(\chi)\, \boldsymbol{\Psi}_{I,v}^{(s)}. \end{cases} \tag{23}$$

By means of relation (9) in Lemma 1, these equations can be stated as follow

$$\begin{cases} u_{s,I}^N(\chi) = \boldsymbol{\Delta}_I(\chi)\, \boldsymbol{P}_I\, \boldsymbol{\Psi}_{I,u}^{(s)}, \\ v_{s,I}^N(\chi) = \boldsymbol{\Delta}_I(\chi)\, \boldsymbol{P}_I\, \boldsymbol{\Psi}_{I,v}^{(s)}. \end{cases} \tag{24}$$

Both approximate solutions will now unify as a vector. Denote $\boldsymbol{Z}_{I,N}^{(s)}(\chi)$ as an approximation to $\boldsymbol{Z}_s(\chi)$ as the true solution of (20). It gives us

$$\boldsymbol{Z}_s(\chi) \approx \boldsymbol{Z}_{I,N}^{(s)}(\chi) := \begin{bmatrix} u_{s,I}^N(\chi) \\ v_{s,I}^N(\chi) \end{bmatrix}. \tag{25}$$

With the aid of former relations (24), we are able to express $\boldsymbol{Z}_{I,N}^{(s)}(\chi)$ in a matrix representations format. We state the next representation, a proof of which is an easy task.

Lemma 2. *In the matrix format, the approximated solution* $\boldsymbol{Z}_{I,N}^{(s)}(\chi)$ *in*

(25) *is expressible as*

$$\boldsymbol{Z}_{I,N}^{(s)}(\chi) = \bar{\boldsymbol{\Delta}}_I(\chi)\,\bar{\boldsymbol{P}}_I\,\bar{\boldsymbol{\Psi}}_I^{(s)}, \tag{26}$$

where

$$\bar{\boldsymbol{\Delta}}_I(\chi) = \begin{bmatrix} \boldsymbol{\Delta}_I(\chi) & \boldsymbol{0} \\ \boldsymbol{0} & \boldsymbol{\Delta}_I(\chi) \end{bmatrix}, \quad \bar{\boldsymbol{P}}_I = \begin{bmatrix} \boldsymbol{P}_I & \boldsymbol{0} \\ \boldsymbol{0} & \boldsymbol{P}_I \end{bmatrix}, \quad \bar{\boldsymbol{\Psi}}_I^{(s)} = \begin{bmatrix} \boldsymbol{\Psi}_{I,u}^{(s)} \\ \boldsymbol{\Psi}_{I,v}^{(s)} \end{bmatrix}.$$

In the next stage we approximate $\frac{d^2}{d\chi^2}\boldsymbol{Z}_s(\chi)$ in the matrix format as available in (23). In the vector format we have to approximate it by

$$\frac{d^2}{d\chi^2}\boldsymbol{Z}_s(\chi) \approx \frac{d^2}{d\chi^2}\boldsymbol{Z}_{I,N}^{(s)}(\chi) := \begin{bmatrix} \ddot{u}_{s,I}^N(\chi) \\ \ddot{v}_{s,I}^N(\chi) \end{bmatrix}. \tag{27}$$

The second-order derivative of $\boldsymbol{Z}_{I,N}^{(s)}(\chi)$ with regard to χ will be now computed by using the relations (24). For this purpose, the only requirement is to calculate the derivatives of $\boldsymbol{\Delta}_I(\chi)$. It can be shown by easy calculations that

$$\frac{d}{d\chi}\boldsymbol{\Delta}_I(\chi) = \boldsymbol{\Delta}_I(\chi)\,\boldsymbol{G}_I, \quad \boldsymbol{G}_I = \begin{bmatrix} 0 & 1 & 0 & \dots & 0 \\ 0 & 0 & 2 & \dots & 0 \\ \vdots & \vdots & 0 & \vdots & \vdots \\ 0 & 0 & 0 & \ddots & I \\ 0 & 0 & 0 & \dots & 0 \end{bmatrix}_{(I+1)\times(I+1)}. \tag{28}$$

By twice differentiation, we reach at

$$\frac{d^2}{d\chi^2}\boldsymbol{\Delta}_I(\chi) = \boldsymbol{\Delta}_I(\chi)\,\boldsymbol{G}_I^2. \tag{29}$$

Two relations (29) and (24) will now be combined to get

$$\begin{cases} \ddot{u}_{s,I}^N(\chi) = \boldsymbol{\Delta}_I(\chi)\,\boldsymbol{G}_I^2\,\boldsymbol{P}_I\,\boldsymbol{\Psi}_{I,u}^{(s)}, \\ \ddot{v}_{s,I}^N(\chi) = \boldsymbol{\Delta}_I(\chi)\,\boldsymbol{G}_I^2\,\boldsymbol{P}_I\,\boldsymbol{\Psi}_{I,v}^{(s)}. \end{cases} \tag{30}$$

Similar to the former Lemma 2, we get the following result for the second-order derivative.

Lemma 3. *In the matrix representation we state the approximated solution* $\frac{d^2}{d\chi^2}\boldsymbol{Z}_{I,N}^{(s)}(\chi)$ *in* (27) *is the form*

$$\frac{d^2}{dx^2}\boldsymbol{Z}_{I,N}^{(s)}(\chi) = \bar{\boldsymbol{\Delta}}_I(\chi)\,\bar{\boldsymbol{G}}_I\,\bar{\boldsymbol{P}}_I\,\bar{\boldsymbol{\Psi}}_I^{(s)}, \tag{31}$$

where $\bar{\boldsymbol{\Psi}}_I^{(s)}$, $\bar{\boldsymbol{\Delta}}_I(\chi)$ *and* $\bar{\boldsymbol{P}}_I$ *are defined in* (26) *and*

$$\bar{\boldsymbol{G}}_I = \begin{bmatrix} \boldsymbol{G}_I^2 & \boldsymbol{0} \\ \boldsymbol{0} & \boldsymbol{G}_I^2 \end{bmatrix}.$$

To continue, we need a set of $(I+1)$ collocation points. There is no rule of thumb for selecting these points. Here, a uniform partitioning of $[0, X]$ into I subintervals with $(I+1)$ partitioning points χ_μ is used to find the coefficients in the series expansion forms (22). Concisely speaking, we set

$$\chi_\mu = \mu X/I, \quad \mu = 0, 1, \ldots, I, \tag{32}$$

as the collocation nodes.

We collocate the matrix equations (20) at these collocation nodes to get

$$\boldsymbol{N}_{s-1,1}(\chi_\mu)\,\frac{d^2}{d\chi^2}\boldsymbol{Z}_s(\chi_\mu) + \boldsymbol{N}_{s-1,2}(\chi_\mu)\,\boldsymbol{Z}_s(\chi_\mu) = \boldsymbol{R}_{s-1}(\chi_\mu),\ \mu = 0, 1, \ldots, I, \tag{33}$$

for $s = 1, 2, \ldots, S$. The goal is to state the foregoing equations in a com-

pact form. In this respect, let us introduce the next matrices and vector

$$\boldsymbol{Q}_{s-1,\ell} = \begin{bmatrix} \boldsymbol{N}_{s-1,\ell}(\chi_0) & \boldsymbol{0} & \dots & \boldsymbol{0} \\ \boldsymbol{0} & \boldsymbol{N}_{s-1,\ell}(\chi_1) & \dots & \boldsymbol{0} \\ \vdots & \vdots & \ddots & \vdots \\ \boldsymbol{0} & \boldsymbol{0} & \dots & \boldsymbol{N}_{s-1,\ell}(\chi_I) \end{bmatrix}, \quad \ell = 1, 2,$$

$$\boldsymbol{F}_{s-1} = \begin{bmatrix} \boldsymbol{R}_{k-1}(\chi_0) \\ \boldsymbol{R}_{k-1}(\chi_1) \\ \vdots \\ \boldsymbol{R}_{k-1}(\chi_I) \end{bmatrix}.$$

We also define the following notations

$$\boldsymbol{W}_s := \begin{bmatrix} \boldsymbol{Z}^{(s)}_{I,N}(\chi_0) \\ \boldsymbol{Z}^{(s)}_{I,N}(\chi_1) \\ \vdots \\ \boldsymbol{Z}^{(s)}_{I,N}(\chi_I) \end{bmatrix} \quad \ddot{\boldsymbol{W}}_s := \begin{bmatrix} \frac{d^2}{d\chi^2}\boldsymbol{Z}^{(s)}_{I,N}(\chi_0) \\ \frac{d^2}{d\chi^2}\boldsymbol{Z}^{(s)}_{I,N}(\chi_1) \\ \vdots \\ \frac{d^2}{d\chi^2}\boldsymbol{Z}^{(s)}_{I,N}(\chi_I) \end{bmatrix}.$$

With the help of matrix and vector notations given above, we recast the set of matrix equations (35) as

$$\boldsymbol{Q}_{s-1,1}\,\ddot{\boldsymbol{W}}_s + \boldsymbol{Q}_{s-1,2}\,\boldsymbol{W}_s = \boldsymbol{F}_{s-1}, \qquad s = 1, 2, \dots, S. \tag{34}$$

The next results provide a matrix format for $\boldsymbol{W}_s$ and $\ddot{\boldsymbol{W}}_s$.

Lemma 4. *If we collocate relations* (26) *and* (31) *at the collocation nodes* (32)*, then one gets the following matrix representations for* $\boldsymbol{W}_s$ *and* $\ddot{\boldsymbol{W}}_s$ *as*

$$\boldsymbol{W}_s = \hat{\bar{\boldsymbol{\Delta}}}_I\,\bar{\boldsymbol{P}}_I\,\bar{\boldsymbol{\Psi}}^{(s)}_I, \qquad \ddot{\boldsymbol{W}}_s = \hat{\bar{\boldsymbol{\Delta}}}_I\,\bar{\boldsymbol{G}}_I\,\bar{\boldsymbol{P}}_I\,\bar{\boldsymbol{\Psi}}^{(s)}_I. \tag{35}$$

Here, two matrices $\bar{\boldsymbol{P}}_I, \bar{\boldsymbol{\Psi}}^{(s)}_I$ *are defined in* (26) *and the block-diagonal matrix* $\bar{\boldsymbol{G}}_I$ *is introduced in* (31)*. Also, we have used*

$$\hat{\bar{\boldsymbol{\Delta}}}_I = [\bar{\boldsymbol{\Delta}}_I(\chi_0) \quad \bar{\boldsymbol{\Delta}}_I(\chi_1) \quad \dots \quad \bar{\boldsymbol{\Delta}}_I(\chi_I)]^t,$$

where the matrix $\bar{\boldsymbol{\Delta}}_I$ *is previously defined in* (26)*.*

By placing two relations (35) into (34) we conclude the next linear fundamental matrix equation

$$\left\{\boldsymbol{Q}_{s-1,1}\,\hat{\bar{\boldsymbol{\Delta}}}_I\,\bar{\boldsymbol{G}}_I+\boldsymbol{Q}_{s-1,2}\,\hat{\bar{\boldsymbol{\Delta}}}_I\right\}\,\bar{\boldsymbol{P}}_I\,\bar{\boldsymbol{\Psi}}_I^{(s)}=\boldsymbol{F}_{s-1},\quad s=1,2,\ldots,S.$$

In an equivalent form we rewrite these equations compactly for $s=1,2,\ldots,S$ as

$$\boldsymbol{A}_s\,\bar{\boldsymbol{\Psi}}_I^{(s)}=\boldsymbol{F}_{s-1},\quad \text{or}\quad [\boldsymbol{A}_s;\boldsymbol{F}_{s-1}],\ \boldsymbol{A}_s:=\left(\boldsymbol{Q}_{s-1,1}\,\hat{\bar{\boldsymbol{\Delta}}}_I\,\bar{\boldsymbol{G}}_I+\boldsymbol{Q}_{s-1,2}\,\hat{\bar{\boldsymbol{\Delta}}}_I\right)\,\bar{\boldsymbol{P}}_I. \tag{36}$$

The implementation of the Neumann boundary conditions (21) into a matrix format is not yet performed and is to be added to the matrix equation (36). Toward this end, we first combine two relations (26) and (28) to obtain

$$\begin{cases}\dot{u}_{s,I}^N(\chi)=\boldsymbol{\Delta}_I(\chi)\,\boldsymbol{G}_I\,\boldsymbol{P}_I\,\boldsymbol{\Psi}_{I,u}^{(s)},\\ \dot{v}_{s,I}^N(\chi)=\boldsymbol{\Delta}_I(\chi)\,\boldsymbol{G}_I\,\boldsymbol{P}_I\,\boldsymbol{\Psi}_{I,v}^{(s)}.\end{cases}$$

By letting χ approaching to $\chi=0,1$ to reach at

$$\begin{aligned}\boldsymbol{A}_s^0\,\bar{\boldsymbol{\Psi}}_I^{(s)}&=\boldsymbol{C}_0^s,\quad \boldsymbol{A}_s^0:=\bar{\boldsymbol{\Delta}}_I(0)\,\bar{\boldsymbol{G}}_I\,\bar{\boldsymbol{P}}_I,\\ \boldsymbol{A}_k^1\,\bar{\boldsymbol{\Psi}}_I^{(s)}&=\boldsymbol{C}_1^s,\quad \boldsymbol{A}_s^1:=\bar{\boldsymbol{\Delta}}_I(1)\,\bar{\boldsymbol{G}}_I\,\bar{\boldsymbol{P}}_I.\end{aligned}$$

To incorporate the boundary conditions, four rows of the fundamental matrix equation $[\boldsymbol{A}_s;\boldsymbol{F}_{s-1}]$ will be substituted by $[\boldsymbol{A}_s^0,\boldsymbol{C}_0^s]$ and $[\boldsymbol{A}_s^1,\boldsymbol{C}_1^s]$. Let us show the modified system by

$$[\check{\boldsymbol{A}}_s;\check{\boldsymbol{F}}_{s-1}],\quad s=1,2,\ldots,S. \tag{37}$$

Based upon solving (37), the unknown Krawtchouk coefficients $\psi_{i,w}^{(s)}$ for $i=0,1,\ldots,I$ and $w=u,v$ will be determined at each time frame s for $s=1,2,\ldots,S$.

In the last stage, the strategy of residual error function (REF) is introduced to measure the accuracy of the presented Taylor-Krawtchouk collocation procedure. This can be achieved by putting the already acquired approximate solutions into (2). Therefore, we arrive at the REFs

in the form

$$\begin{bmatrix} \mathrm{Res}_{u,I}^{(s)}(\chi) \\ \mathrm{Res}_{v,I}^{(s)}(\chi) \end{bmatrix} = \left| \boldsymbol{N}_{s-1,1}(\chi) \frac{d^2}{d\chi^2} \boldsymbol{Z}_{I,N}^{(s)}(\chi) + \boldsymbol{N}_{s-1,2}(\chi) \boldsymbol{Z}_{I,N}^{(s)}(\chi) - \boldsymbol{R}_{s-1}(\chi) \right| \cong 0, \tag{38}$$

for $s = 1, 2, \ldots, S$. We note that the true solution of the auto-catalytic system is not available in general. In this case, the technique of REFs will be very useful to testify the performance of the Taylor-Krawtchouk matrix algorithm.

5 Simulation results

The performance of the Taylor-Krawtchouk matrix collocation method is now tested through doing numerical computations for the system (2). Some numerical test cases using diverse model parameters validate the presented combined Taylor-Krawtchouk algorithm and describe the accuracy through tabulated results and graphical representations. Matlab software program version R2021a used to implement the proposed combined numerical algorithm on a personal laptop.

Example 1. We take the following initial conditions for the auto-catalytic glycosis system (2) in the form [6]

$$f(\chi) = \frac{7}{2} + \frac{1}{10} \sin \chi, \quad g(\chi) = \frac{28}{100} + \frac{1}{10} \sin \chi,$$

and the zero Neumann boundary conditions (4) are set at the endpoints of $D = (0, 1)$. The following parameters as the coefficients of the model are taken

$$d_u = d_v = 0.001, \quad \sigma = 3.5, \quad \lambda = 2.5.$$

Let us take $I = 5$. The parameter $N = 2$ is taken in the used Krawtchouk polynomials. We also utilize $h = 0.125$ and $T = 100$. By using the aforementioned parameters in the Taylor-Krawtchouk method

at the first time level $\tau = h$ and $\tau = T/2$ are given respectively by

$$u^2_{1,5}(\chi) = -2.1446\,\chi^5 + 5.82878\,\chi^4 - 5.63083\,\chi^3 + 2.15018\,\chi^2 + 3.30033,$$
$$v^2_{1,5}(\chi) = 0.161379\,\chi^5 - 0.432139\,\chi^4 + 0.40765\,\chi^3 - 0.150649\,\chi^2 + 0.0318,$$

and

$$\begin{aligned} u^2_{400,5}(\chi) &= -2.33 \times 10^{-23}\,\chi^5 + 7.65 \times 10^{-23}\,\chi^4 - 9.25 \times 10^{-23}\,\chi^3 \\ &\quad + 4.41 \times 10^{-23}\,\chi^2 + 1.80 \times 10^{-130}\,x + 0.247844, \\ v^2_{400,5}(\chi) &= -2.25 \times 10^{-26}\,\chi^5 + 7.28 \times 10^{-26}\,\chi^4 - 8.65 \times 10^{-26}\,\chi^3 \\ &\quad + 4.05 \times 10^{-26}\,\chi^2 - 3.52 \times 10^{-133}\,x + 0.0701966. \end{aligned}$$

The obtained approximations at the last level $\tau = T$ are as follow

$$\begin{aligned} u^2_{800,5}(\chi) &= -3.78 \times 10^{-46}\,\chi^5 + 1.90 \times 10^{-45}\,\chi^4 - 3.82 \times 10^{-45}\,\chi^3 \\ &\quad + 2.88 \times 10^{-45}\,\chi^2 + 0.247844, \\ v^2_{800,5}(\chi) &= -3.44 \times 10^{-49}\,\chi^5 + 1.71 \times 10^{-48}\,\chi^4 - 3.40 \times 10^{-48}\,\chi^3 \\ &\quad + 2.55 \times 10^{-48}\,\chi^2 - 4.66 \times 10^{-156}\,x + 0.0701966. \end{aligned}$$

Figure. 1 presents the profile of the approximate solutions using the above mentioned parameters on the space-time domain $[0, 1] \times [0, 100]$. While the left picture shows the concentration u, the right plot displaces the concentration v graphically. A 2D representations of the concentrations at $\chi = 0.8$ and for all $\tau \in [0, 100]$ are further shown in Fig. 2. A 3D snapshots of the achieved REFs obtained via (38) are also depicted in Fig. 3 at different time level $\tau = \tau_s$ for $s = 1, 2, \ldots, 800$. Note that the obtained results are completely matched with those outcomes obtained by the two finite difference methods (FDMs) namely the explicit Euler and the implicit Crank-Nicolson approaches developed in [6]. The same conclusion can be made by comparison the results by those reported by the positivity preserving nonstandard FDMs based on the splitting technique investigated in [5]. Also note that the numerical solutions obtained by the Taylor-Krawtchouk method converge to the equilibrium point $(u_*, v_*) = (\lambda, \frac{\lambda}{\lambda^2+\sigma}) = (0.25, 0.0702)$, which is stable due to the fact that $\kappa = -4.5274$

is negative.

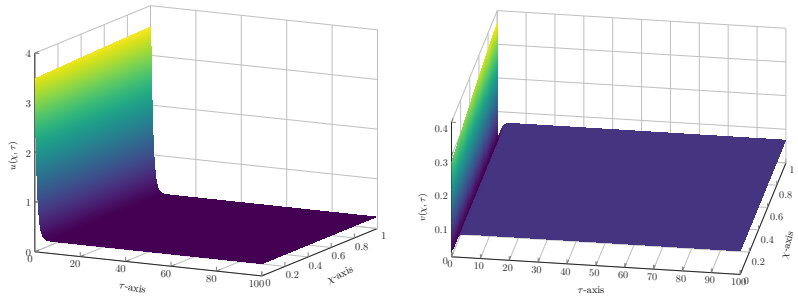

Figure 1. Graphing of approximate solutions $u(\chi, \tau)$ (left) and $v(\chi, \tau)$ (right) via Taylor-Krawtchouk algorithm in Example 1 with $I = 5$, $N = 2$, $h = 0.125$, for $(\chi, \tau) \in [0, 1] \times [0, 100]$.

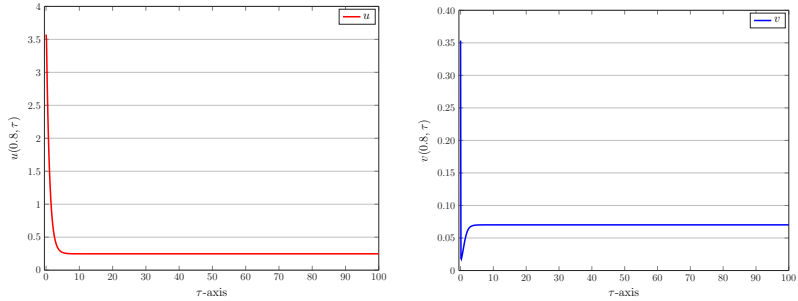

Figure 2. Graphing of concentrations via Taylor-Krawtchouk algorithm in Example 1 with $I = 5$, $N = 2$, $h = 0.125$ at $\chi = 0.8$.

Example 2. Here, we utilize the same initial conditions as given in Example 1. However, the following different parameters will be used in computations as

$$d_u = d_v = 0.001, \quad \sigma = 0.008, \quad \lambda = 0.6.$$

We emphasize that these values of λ and σ selected to ensure that the value of $\kappa = 0.5885$ is positive, thus the equilibrium point is unstable.

In this case, let us employ $I = 5$ and $T = 100$ in the computations. We take $N = 1$ in the basis functions and the time step size is $h = 0.025$.

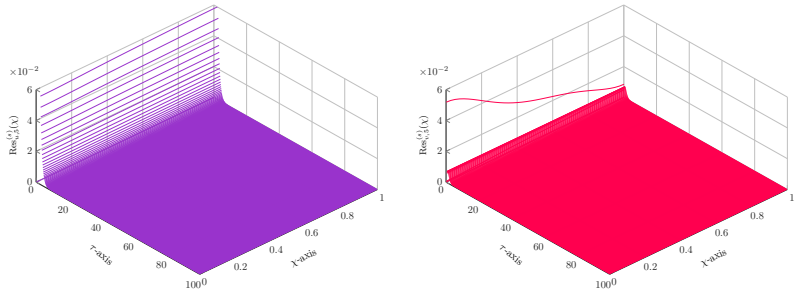

Figure 3. Graphing of REFs $\mathrm{Res}_{u,5}^{(s)}(\chi)$ (left) and $\mathrm{Res}_{v,I}^{(s)}(\chi)$ (right) achieved via Taylor-Krawtchouk algorithm in Example 1 with $I = 5$, $N = 2$, $h = 0.125$, for $s = 1, 2, \ldots, 800$.

The polynomials solutions at time frames $\tau = h$, $\tau = T/2$, and $\tau = T$ are given respectively by

$$u_{1,5}^{1}(\chi) = -1.21485\,\chi^5 + 3.30763\,\chi^4 - 3.20271\,\chi^3 + 1.22593\,\chi^2 + 3.43642,$$
$$v_{1,5}^{1}(\chi) = -0.70125\,\chi^5 + 1.91237\,\chi^4 - 1.8564\,\chi^3 + 0.713003\,\chi^2 + 0.20942,$$

$$\begin{aligned} u_{2000,5}^{1}(\chi) &= 0.00190182\,\chi^5 - 0.00458962\,\chi^4 - 0.000486017\,\chi^3 \\ &\quad + 0.00515372\,\chi^2 + 0.122532, \\ v_{2000,5}^{1}(\chi) &= -0.010172\,\chi^5 + 0.0239476\,\chi^4 + 0.00488162\,\chi^3 - 0.0297876\,\chi^2 \\ &\quad + 1.47497, \end{aligned}$$

and

$$\begin{aligned} u_{4000,5}^{1}(\chi) &= -0.000024923\,\chi^5 + 0.000056981\,\chi^4 + 0.00001841\,\chi^3 \\ &\quad - 0.000079276\,\chi^2 + 0.029158, \\ v_{4000,5}^{1}(\chi) &= -0.00628244\,\chi^5 + 0.0146792\,\chi^4 + 0.00341553\,\chi^3 \\ &\quad - 0.0187755\,\chi^2 + 3.74061, \end{aligned}$$

The graphical representations of two concentrations are visualized on Fig. 4 on the whole domain $(x, \tau) \in [0, 1] \times [0, 100]$. The profile of these quantities at $\chi = 0.8$ and for $\tau \in [0, 100]$ are depicted on Fig. 5. By looking at the

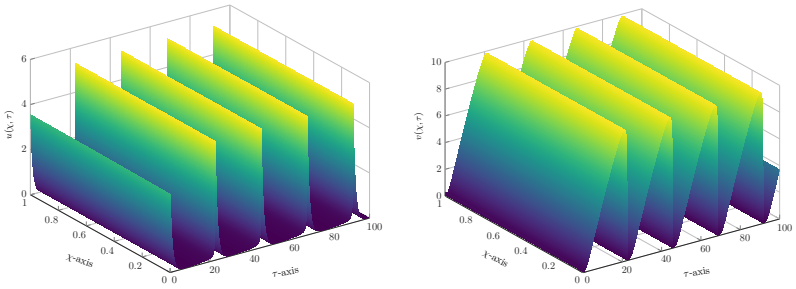

Figure 4. Graphing of approximate solutions $u(\chi,\tau)$ (left) and $v(\chi,\tau)$ (right) via Taylor-Krawtchouk algorithm in Example 2 with $I = 5,\ N = 1,\ h = 0.025$, for $(\chi,\tau) \in [0,1] \times [0,100]$.

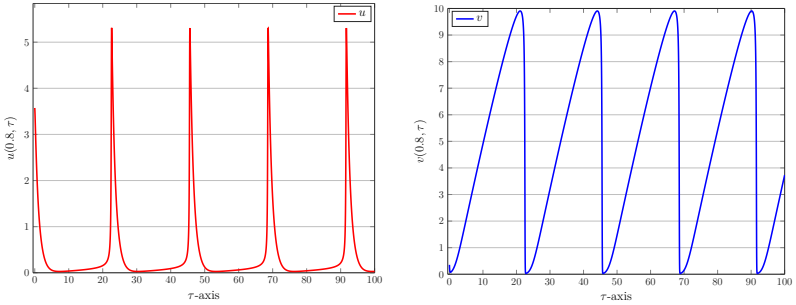

Figure 5. Graphing of concentrations via Taylor-Krawtchouk algorithm in Example 2 with $I = 5,\ N = 1,\ h = 0.025$ at $\chi = 0.8$.

plotted Figs. 4 and 5 we infer that under the condition $\kappa > 0$ the behavior of both concentrations $u(\chi,\tau)$ and $v(\chi,\tau)$ are unstable and these results are consistent with the continuous glycolysis model.

Example 3. Let us take different initial conditions from those given in Example 1 and 2 in the forms [35]

$$f(\chi) = \frac{5}{10} + \frac{1}{10}\sin\chi, \quad g(\chi) = \frac{1429}{1000} + \frac{1}{10}\sin\chi,$$

We further set different values of diffusion parameters will be used in computations as

$$d_u = 1, \quad d_v = 0.8, \quad \sigma = 0.1, \quad \lambda = 0.5.$$

With the above model parameters σ and λ, we have $\kappa = 0.0786$, which implies that the equilibrium point (u_*, v_*) is unstable point for the system.

To get a polynomial solution for the model (2) under the above-mentioned parameters, we set $I = 5$ and $T = 100$. In the Krawtchouk bases we set $N = 1$ and the time step size is taken as $h = 0.5$. Let us consider the obtained approximate solutions at time frames $\tau = h$ and $\tau = T$. These approximations are as follow:

$$u^1_{1,5}(\chi) = -0.0017673\,\chi^5 + 0.0082890\,\chi^4 - 0.031726\,\chi^3 + 0.035429\,\chi^2 + 0.42148,$$

$$v^1_{1,5}(\chi) = -0.00463771\,\chi^5 + 0.0152208\,\chi^4 - 0.0332002\,\chi^3 + 0.030953\,\chi^2 + 1.4663,$$

and

$$\begin{aligned} u^1_{200,5}(\chi) &= 1.0980 \times 10^{-5}\,\chi^5 - 2.9737 \times 10^{-5}\,\chi^4 + 2.7196 \times 10^{-5}\,\chi^3 \\ &\quad - 8.7703 \times 10^{-6}\,\chi^2 + 0.359169, \\ v^1_{200,5}(\chi) &= 5.1055 \times 10^{-7}\,\chi^5 - 1.3827 \times 10^{-6}\,\chi^4 + 1.2645 \times 10^{-6}\,\chi^3 \\ &\quad - 4.0780 \times 10^{-7}\,\chi^2 + 2.18338. \end{aligned}$$

In addition to these two frames, let us plot the approximate solutions in all time frames $\tau = \tau_s h$, $0 \leqslant s \leqslant 200$. These approximations are displayed in Fig. 6 for both solutions $u(\chi, \tau)$ and $v(\chi, \tau)$ in the space-time domain $[0, 1] \times [0, 100]$. The snapshots of approximate solutions evaluated at $\chi = 0.8$ are also depicted in the next Fig. 7. In terms of achieved REFs, we further visualize the corresponding obtained errors at $\chi = 0.8$ on the same figure. It can be clearly detected that the proposed Taylor-Krawtchouk algorithm produces positive values of concentrations for both u and v. The plotted figures imply that the produced approximations are consistent with the continuous glycolysis model and preserve all important properties of the underlying model problem (2).

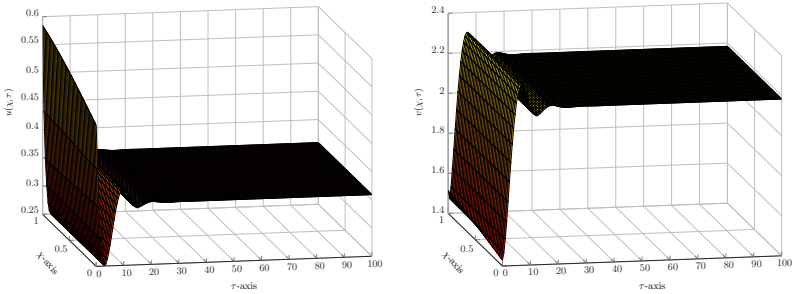

Figure 6. Graphing of approximate solutions $u(\chi, \tau)$ (left) and $v(\chi, \tau)$ (right) via Taylor-Krawtchouk algorithm in Example 3 with $I = 5,\ N = 1,\ h = 0.5$, for $(\chi, \tau) \in [0, 1] \times [0, 100]$.

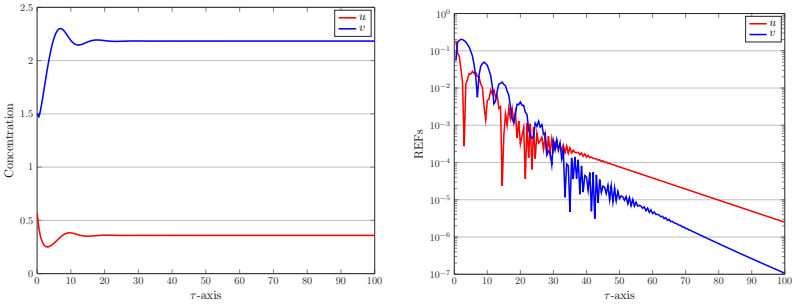

Figure 7. Graphing of concentrations (left) and the associated REFs (right) via Taylor-Krawtchouk algorithm in Example 3 with $I = 5,\ N = 1,\ h = 0.5$ at $\chi = 0.8$.

6 Conclusions

In this work, we setup a combined numerical procedure based on Taylor time-marching and the spectral matrix collocation algorithm based on the novel Krawtchouk polynomials to solve the glycolysis reaction-diffusion (RD) system arising in mathematical chemistry. The inherent nonlinearity of the given system of PDEs was first tackled by using the Taylor time advancement procedure. Then, in each time frame we solved the resulting family of system of linear ODEs by utilizing the spectral Krawtchouk matrix collocation algorithm. We mathematically proved that the sequence of Krawtchouk bases convergent in a weighed L_2 norm. By performing some computational experiments we numerically confirmed that the pro-

posed Taylor-Krawtchouk technique is dynamically consistent with respect to positivity property of the chemical concentrations. By employing the present combined approach and in comparison with existing numerical procedures, the solution of a glycolysis RD system is easily obtained and the computational algorithm is greatly simplified.

References

[1] M. A. Abdelkawy, H. Ahmad, M. B. Jeelani, A. S. Alnahdi, Fully Legendre spectral collocation technique for stochastic heat equations, *Open Phys.* **19** (2021) 921–931.

[2] G. Adomian, The diffusion-Brusselator equation, *Comput. Math. Appl.* **59** (1995) 1–3.

[3] N. Ahmed, D. Baleanu, A. Korkmaz, M. Rafiq, M. A. Rehman, M. Ali, Positivity preserving computational techniques for nonlinear autocatalytic chemical reaction model, *Rom. Rep. Phys.* **72** (2020) #121.

[4] S. Ahmed, S. Jahan, K. S. Nisar, Hybrid Fibonacci wavelet method to solve fractional-order logistic growth model, *Math. Methods Appl. Sci.* **46** (2023) 16218–16231.

[5] N. Ahmed, M. Rafiq, D. Baleanu, M. A. Rehman, I. Khan, M. Ali, K. S. Nisar, Structure preserving algorithms for mathematical model of auto-catalytic glycolysis chemical reaction and numerical simulations, *Eur. Phys. J. Plus* **135** (2020) #522.

[6] N. Ahmed, S. S. Tahira, M. Imran, M. Rafiq, M. A. Rehman, M. Younis, Numerical analysis of auto-catalytic glycolysis model, *AIP Adv.* **9** (2019) #085213.

[7] M. Best, *A Contribution to the Nonexistence of Perfect Codes*, Ph.D. thesis, University of Amsterdam, 1982.

[8] Y. M. Chu, N. A. Shah, H. Ahmad, J. D. Chung, S. M. Khaled, A comparative study of semi-analytical methods for solving fractional-order Cauchy reaction-diffusion equation, *Fractals* **29** (2021) #2150143.

[9] P. Gray, S. K. Scott, Autocatalytic reactions in the isothermal, continuous stirred tank reactor: isolas and other forms of multistability, *Chem. Eng. Sci.* **38** (1983) 29–43.

[10] P. Gray, S. K. Scott, Autocatalytic reactions in the isothermal, continuous stirred tank reactor: oscillations and instabilities in the system $A + 2B \to 3B$, $B \to C$, *Chem. Eng. Sci.* **39** (1984) 1087–1097.

[11] G. Hu, Z. Qiao, T. Tang, Moving finite element simulations for reaction-diffusion systems, *Adv. Appl. Math. Mech.* **4** (2012) 365–381.

[12] C. Ivan, A multidimensional nonlinear growth, birth and death, emigration and immigration process, in: *Proceedings of the Fourth Conference on Probability Theory (Brasov,1971)*, Editura Acad. R. S. R., Bucharest, 1973, pp. 421–427.

[13] M. Izadi, P. Roul, A new approach based on shifted Vieta-Fibonacci-quasilinearization technique and its convergence analysis for nonlinear third-order Emden-Fowler equation with multi-singularity, *Commun. Nonlin. Sci. Num. Simul.* **117** (2023) #106912.

[14] M. Izadi, J. Singh, S. Noeiaghdam, Simulating accurate and effective solutions of some nonlinear nonlocal two-point BVPs: Clique and QLM-clique matrix methods, *Heliyon* **9** (2023) #e22267.

[15] M. Izadi, H. M. Srivastava, Fractional clique collocation technique for numerical simulations of fractional-order Brusselator chemical model, *Axioms* **11** (2022) #654.

[16] M. Izadi, H. M. Srivastava, The reaction-diffusion models in biomedicine: Highly accurate calculations via a hybrid matrix collocation algorithm, *Appl. Sci.* **13** (2023) #11672.

[17] Izadi M, S. Yüzbası, W. Adel, Accurate and efficient matrix techniques for solving the fractional Lotka-Volterra population model, *Physica A* **600** (2022) #127558.

[18] A. Korkmaz, O. Ersoy, I. Dag, Motion of patterns modeled by the Gray-Scott autocatalysis system in one dimension, *MATCH Commun. Math. Comput. Chem.* **77** (2017) 507–526.

[19] I. Krasikov, S. Litsyn, On integral zeros of Krawtchouk polynomials, *J. Comb. Theory Ser. A* **74** (1996) 71–99.

[20] V. Levenshtein, Krawtchouk polynomials and universal bounds for codes and designs in Hamming spaces, *IEEE Trans. Inf. Theory* **41** (1995) 1303–1321.

[21] R. E. Mickens, Positivity preserving discrete model for the coupled ODE's modeling glycolysis, in: *Proceeding of the Fourth International*

Conference on Dynamical Systems and Differential Equations, Wilmington, 2002, pp. 623–629.

[22] R. C. Mittal, R. Jiwari, Numerical solution of two-dimensional reaction-diffusion Brusselator system, *Appl. Math. Comput.* **217** (2011) 5404–5415.

[23] G. Nicolis, I. Prigogine, *Self-Organization in Nonequilibrium Systems*, Wiley, New York, 1977.

[24] W. Y. Qiu, R. Wong, Asymptotic expansion of the Krawtchouk polynomials and their zeros, *Comput. Methods Func. Theory* **4** (2004) 189–226.

[25] M. Razavi, M. M. Hosseini, A. Salemi, Error analysis and Kronecker implementation of Chebyshev spectral collocation method for solving linear PDEs, *Comput. Methods Diff. Eq.* **10** (2022) 914–927.

[26] A. H. Romano, T. Conway, Evolution of carbohydrate metabolic pathways, *Res. Microbio.* **147** (1996) 448–455.

[27] E. E. Sel'Kov, Self-oscillation in glycolysis. 1. A simple model, *Eur. J. Biochem.* **4** (1968) 79–86.

[28] H. M. Srivastava, M. Izadi, Generalized shifted airfoil polynomials of the second kind to solve a class of singular electrohydrodynamic fluid model of fractional order, *Fractal Fract.* **7** (2023) #7.

[29] H. M. Srivastava, H. L. Manocha, *A Treatise on Generating Functions*, Halsted Press, New York, 1984.

[30] S. H. Strogatz, *Nonlinear Dynamics and Chaos with Applications to Physics, Biology, Chemistry, and Engineering*, Adisson-Wesley, New York, 1994.

[31] V. M. Tripathi, H. M. Srivastava, H. Singh, C. Swarup, S. Aggarwal, Mathematical analysis of non-isothermal reaction-diffusion models arising in spherical catalyst and spherical biocatalyst, *Appl. Sci.* **11** (2021) #10423.

[32] E. H. Twizell, A. B. Gumel, Q. Cao, A second order scheme for the Brusselator reaction–diffusion system, *J. Math. Chem.* **26** (1999) 297–316.

[33] M. Wei, J. Wu, G. Guo, Steady state bifurcations for a glycolysis model in biochemical reaction, *Nonlin. Anal. Real World Appl.* **22** (2015) 155–175.

[34] Y. H. Youssri, W. M. Abd-Elhameed, H. M. Ahmed, New fractional derivative expression of the shifted third-kind Chebyshev polynomials: Application to a type of nonlinear fractional pantograph differential equations, *J. Func. Spaces* **2022** (2022) #3966135.

[35] J. Zhou, J. Shi, Pattern formation in a general glycolysis reaction-diffusion system, *IMA J. Appl. Math.* **80** (2015) 1703–1738.